

# Integrated microfluidic variable optical attenuator

Lin Zhu, Yanyi Huang, and Amnon Yariv

Department of Electrical Engineering and Department of Applied Physics, California Institute of Technology  
Pasadena, California 91125

[linz@caltech.edu](mailto:linz@caltech.edu)

**Abstract:** We fabricate and measure a microfluidic variable optical attenuator which consists of an optical waveguide integrated with a microfluidic channel. An opening is introduced in the upper cladding of the waveguide in order to facilitate the alignment and bonding of the microfluidic channel. By using fluids with different refractive indices, the optical output power is gradually attenuated. We obtain a maximum attenuation of 28 dB when the fluid refractive index changes from 1.557 to 1.584.

©2005 Optical Society of America

OCIS codes: (130.3120) Integrated optics devices; (230.3990) Microstructure devices

---

## References and links

1. B. Barber, C. R. Giles, V. Askyuk, R. Ruel, L. Stulz, and D. Bishop, "A fiber connectorized MEMS variable optical attenuator," *IEEE Photonics Technol. Lett.* **10**, pp. 1262-1264 (1998).
2. X. M. Zhang, A. Q. Liu, C. Lu, and D. Y. Tang, "MEMS variable optical attenuator using low driving voltage for DWDM systems," *Electron. Lett.* **38**, pp. 382-383 (2002).
3. T. Kawai, M. Koga, M. Okuno, and T. Kitoh, "PLC type compact variable optical attenuator for photonic transport network," *Electron. Lett.* **34**, pp. 264-265 (1998).
4. M. Lenzi, S. Tebaldini, D. D. Mola, S. Brunazzi, and L. Cibinetto, "Power control in the photonic domain based on integrated arrays of optical variable attenuators in glass-on-silicon technology," *IEEE J. Sel. Top. Quantum Electron.* **5**, pp. 1289-1297 (1999).
5. G. Z. Xiao, Z. Zhang, and C. P. Grover, "A variable optical attenuator based on a straight polymer-silica hybrid channel waveguide," *IEEE Photonics Technol. Lett.* **16**, pp. 2511-2513 (2004).
6. C. Kerbage, R. S. Windeler, B. J. Eggleton, P. Mach, M. Dolinski, and J. A. Rogers, "Tunable devices based on dynamic positioning of micro-fluids in micro-structured optical fiber," *Opt. Commun.* **204**, pp. 179-184 (2002).
7. C. Kerbage, A. Hale, A. Yablon, R. S. Windeler, and B. J. Eggleton, "Integrated all-fiber variable attenuator based on hybrid microstructure fiber," *Appl. Phys. Lett.* **79**, pp. 3191-3193 (2004).
8. P. Mach, M. Dolinski, K. W. Baldwin, J. A. Rogers, C. Kerbage, R. S. Windeler, B. J. Eggleton, "Tunable microfluidic optical fiber," *Appl. Phys. Lett.* **80**, pp. 4294-4296 (2004).
9. C. Grillet, P. Domachuk, V. Ta'eed, E. Magi, J. A. Bolger, B. J. Eggleton, L. E. Rodd, and J. Cooper-White, "Compact tunable microfluidic interferometer," *Opt. Express* **12**, pp. 5440-5447 (2004).  
<http://www.opticsexpress.org/abstract.cfm?URI=OPEX-12-22-5440>
10. P. Domachuk, M. Cronin-Golomb, B. J. Eggleton, S. Mutzenich, G. Rosengarten, and A. Mitchell, "Application of optical trapping to beam manipulation in optofluidics," *Opt. Express* **13**, pp. 7265-7275 (2005).  
<http://www.opticsexpress.org/abstract.cfm?URI=OPEX-13-19-7265>
11. A. Y. Fu, C. Spence, A. Scherer, F. H. Arnold, and S. R. Quake, "A microfabricated fluorescence-activated cell sorter," *Nature Biotechnology* **17**, pp. 1109-1111 (1999).
12. S. Balslev and A. Kristensen, "Microfluidic single-mode laser using high-order Bragg grating and antiguiding segments," *Opt. Express* **13**, pp. 344-351 (2005).  
<http://www.opticsexpress.org/abstract.cfm?URI=OPEX-13-1-344>
13. M. L. Adams, M. Loncar, A. Scherer, and Y. Qiu, "Microfluidic integration of porous photonic crystal nanolasers for chemical sensing," *IEEE J. Sel. Top. Quantum Electron.* **23**, pp. 1348-1354 (2005).
14. J. M. Ruano, V. Benoit, J. S. Aitchison, and J. M. Cooper, "Flame hydrolysis deposition of glass on silicon for the integration of optical and microfluidic devices," *Anal. Chem.* **72**, pp. 1093-1097 (2000).
15. P. Friis, K. Hoppe, O. Leistiko, K. B. Mogensen, J. Hubner, and J. P. Kutter, "Monolithic integration of microfluidic channels and optical waveguides in silica on silicon," *Appl. Opt.* **40**, pp. 6246-6251 (2001).

16. V. Lien, Y. Berdichevsky, and Y. Lo, "A prealigned process of integrating optical waveguides with microfluidic devices," *IEEE Photonics Technol. Lett.* **16**, pp. 1525-1527 (2004).
  17. Y. Xia and G. M. Whitesides, "Soft lithography," *Annu. Rev. Mater. Sci.* **28**, pp. 153-184 (1998).
  18. Y. Huang, G.T. Paloczi, J. K. S. Poon, and A. Yariv, "Bottom-up soft-lithographic fabrication of three-dimensional multilayer polymer integrated optical microdevices," *Appl. Phys. Lett.* **85**, pp. 3005-3007 (2004).
- 

## 1. Introduction

Integrated tunable variable optical attenuators (VOA) are widely used for the monitoring and active control of optical channel power in modern high speed optical wavelength division multiplexed (WDM) networks. There are two main implementations of VOA: micro-electro mechanical systems (MEMS) based and planar lightwave circuit (PLC) based. In MEMS, several electrically driven mirrors are placed along the optical path to control the power attenuation by changing the mirror reflection angles and directions [1, 2]. The main problem with this method is the reliability and integration with other planar optical structures. In PLC, the thermo-optic effect is used to tune the refractive index of the waveguide material, thus changing the optical confinement of a waveguide core or the phase difference between two branches of an interferometer [3-5]. The specific PLC can be a straight channel waveguide, waveguide bend or Mach-Zehnder interferometer. The main concern for this method includes material selection, dimension stability under high temperatures and power consumption. Microfluidic methods have been used for the optical intensity and phase modulation in micro-structure fibers [6-8] and optical interferometers [9, 10]. In this letter, we demonstrate an integrated microfluidic method to tune the attenuation of optical waveguides in a planar platform, using fluids with different refractive indices flowing in a microfluidic channel as the cladding for a segment of straight optical waveguide.

Recently, the integration of optics and microfluidics has attracted much attention and is widely used for microfluidic dye lasers, optical sensing, and biological detection [11-13]. Monolithic integration of a planar optical waveguide with a microfluidic channel is particularly important because it combines two basic elements of optical and microfluidic devices. Until now, this integration mainly focused on inserting a microfluidic channel between two segments of a split waveguide core in a coplanar topology, where optics part is used for the fluorescence detection or biochemical sensing. It has been demonstrated in a silica-on-silicon structure with reactive ion etching and oxide deposition process [14, 15] and in a Polydimethylsiloxane (PDMS) material system with a prealigned method [16].

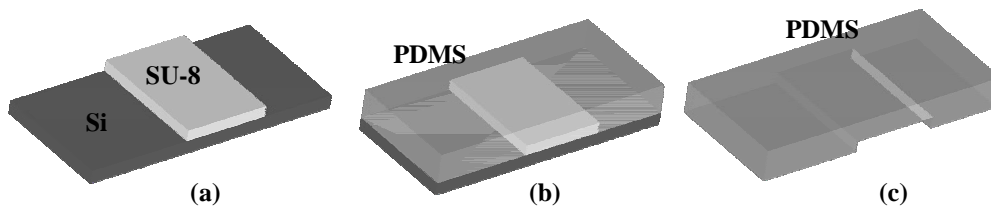
In this letter, we adopt a different approach, by aligning the microfluidic channel on an opening in the cladding layer [Fig. 1(g)]. The fluid in the channel acts as a segment of upper cladding and creates a hybrid fluid-solidstate waveguide structure. Compared to the integration scheme proposed in the past, our design keeps the waveguide core intact and confines the interaction between the fluids and optical waveguides within the cladding layer. This layout is suitable for applications where the microfluidics serve as a tunable upper cladding.

## 2. Microfluidic VOA fabrication process

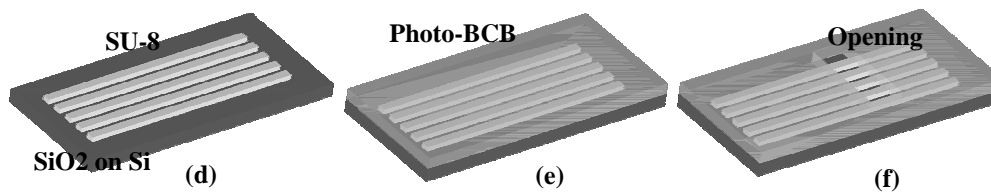
The schematic of the fabrication procedure of the device is shown in Fig. 1. In the first main step, the PDMS microfluidic channel is fabricated using a standard soft lithography process, where the channel is the negative relief of the master device [17, 18]. The master structure [Fig. 1(a)] in our demonstration is made of SU-8 2025 (Microchem), a negative photoresist. A 40  $\mu\text{m}$  thick SU-8 layer is first spun on a silicon wafer and the pattern is defined using photolithography. The PDMS prepolymer (RTV-615 kit, GE) is poured on the master chip and cured [Fig. 1(b)]. After cooling down to room temperature, the cured PDMS layer is peeled off to serve as the microfluidic channel [Fig. 1(c)]. The length and width of the channel are 2 mm and 0.4mm, respectively.

In the second main step, the optical device is fabricated by a multistep photolithography process. First, the waveguide core [Fig. 1(d)] is formed by photolithography on a 1.8  $\mu\text{m}$  thick SU-8 2002 (Microchem) layer on a silicon wafer with 5  $\mu\text{m}$  of thermally grown silicon oxide, which serves as the lower cladding. Then a 4.2  $\mu\text{m}$  thick upper cladding layer of photosensitive benzocyclobutene (Photo-BCB) (CYCLOTENE 4022-35, Dow) is spun on the substrate with the waveguides [Fig. 1(e)]. After the Photo-BCB is pre-baked, a 300  $\mu\text{m}$  long and 100 $\mu\text{m}$  wide window is opened on a segment of waveguide core by a second UV photolithography through a photomask [Fig. 1(f)]. The chip is finally baked at 250 $^{\circ}\text{C}$  for an hour. The baking step is important for completely curing the material and defining the refractive index contrast since the post-baking changes the refractive index of both the SU-8 and Photo-BCB. We choose processing parameters carefully to ensure good waveguide quality without damaging polymer materials under high temperatures, resulting in a core index of 1.561 and cladding index of 1.546. The refractive index numbers are obtained from the numerical fitting between the measurement results and the simulation results.

### I PDMS Microfluidic Channel



### II Waveguide and Cladding Patterning



### III Microfluidic Channel Waveguide Alignment

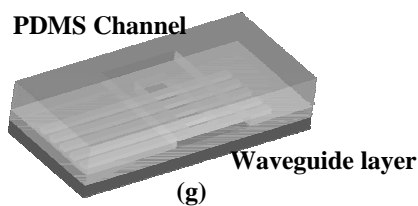


Fig. 1. Schematic flowchart for the fabrication of an integrated microfluidic variable optical attenuator. The sequential steps are labeled from (a) to (g).

The final step is the bonding of the microfluidic channel to the optical chip. To facilitate the bonding, a high power oxygen plasma treatment is used to activate the surface of both the PDMS channel and Photo-BCB cladding. The plasma exposure is 30 seconds long at an RF power of 80W and O<sub>2</sub> pressure of 200mTorr. Then the PDMS channel is aligned with the opening on the chip under an optical microscope by hand [Fig. 1(g)]. The final device is baked at 80 $^{\circ}\text{C}$  for 8 hours in an oven to ensure good adhesion between the PDMS and Photo-BCB. Figure 2 shows an optical and a scanning electron micrograph of a fabricated device.

Our processing method has several advantages for the fabrication of integrated optical microfluidic devices. First, the process is based on photolithography and soft lithography, which are cost effective and scalable to mass production. Second, problems of the alignment and adhesion of the microfluidic layer to the optical layer, which are crucial for microfluidic optical device integration, are successfully solved in our approach. The size of the microfluidic channel and cladding opening is on the order of  $100\ \mu\text{m}$ , so the alignment does not require a high degree of accuracy. The good adhesion between the PDMS channel and Photo-BCB cladding, which is enabled by the buried nature of the waveguide core, prevents possible fluid leakage problems. The buried waveguide core also provides mechanical stability. Lastly, the two negative resists, SU-8 and Photo-BCB, are chemically inert when cured, making the device ideal for microfluidic applications, where various liquids may contact the SU-8 and Photo-BCB. We can also use this architecture for refractive index sensing and complex planar waveguide structures.

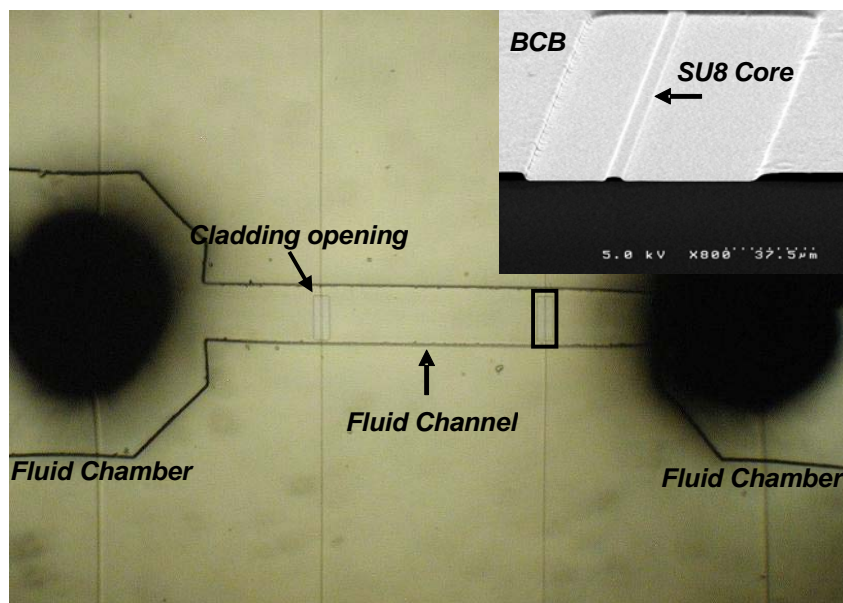


Fig. 2. The optical image shows the integrated microfluidic optical chip and the inset SEM image shows SU-8 waveguide core embedded in the window opening of the BCB cladding. Two pin holes in the fluid chambers part on the microfluidic layer serve as fluid input and output ports. From the inset, the height of the SU-8 waveguide core and BCB cladding are  $1.8\ \mu\text{m}$  and  $4.2\ \mu\text{m}$ , respectively.

### 3. Experiment results and discussions

To operate the device, we flow fluids with different refractive indices through the microfluidic channel to tune the optical confinement of the waveguide. The fluids are externally injected into the channel through a syringe mounted on a syringe pump. When the refractive index of the fluid equals the waveguide cladding, the device is equivalent to a uniform waveguide, giving the maximum optical power output. The output power is attenuated when we use a fluid with a refractive index higher than the waveguide core. Thus, fluids with accurate refractive indices of suitable range are important to the operation of our device. In our experiment, we use index matching fluids from Cargille Labs, which provide an index range of 1.4-1.7 with a step of 0.001.

In Fig. 3, the dotted line shows the numerical simulation result for the fabricated device based on a beam propagation method (BPM). We only consider the portion of the waveguide with the cladding opening and assume a rectangle waveguide core cross-section for simplicity.

The refractive indices of the substrate is 1.440, corresponding to silica. The height and width of the waveguide core is 1.8  $\mu\text{m}$  and 5.2  $\mu\text{m}$ , respectively. The total length for the simulation is 300  $\mu\text{m}$ . The result is the average of TE and TM polarization input. We can find the power attenuation is more than 30 dB for the simulated structure when the cladding index changes from 1.555 to 1.585. On average, a change in refractive index of 0.001 causes an attenuation around 1 dB. These specifications satisfy most applications with VOA [5].

For the measurement of the fabricated device, a tunable laser provides optical input signal with the wavelength of 1.55  $\mu\text{m}$  through a paddle polarization controller or a polarization scrambler. The light is coupled into one end of the device using a tapered fiber. The output optical signal, collected by a multimode fiber from the other end facet of the device, is measured by an infrared optical power meter. The background noise floor limits minimum measurable optical power attenuation to around 32 dB. In Fig. 3, the solid line shows the measured attenuation. We scramble the polarization state of the input light to obtain an average result among all polarization states. The measurement result agrees very well with the simulation result for the power attenuation. The maximum attenuation is about 28dB when the fluid refractive index changes from 1.557 to 1.584. The measured optical power increases when the fluid index changes from 1.500 to 1.546, the refractive index of the Photo-BCB. The reason is that when the fluid refractive index does not match the BCB cladding, optical reflection is present at two interfaces between the cladding opening and the Photo-BCB cladding. The reflection becomes weaker, resulting in the increase of output power, as the fluid index approaches the cladding index.

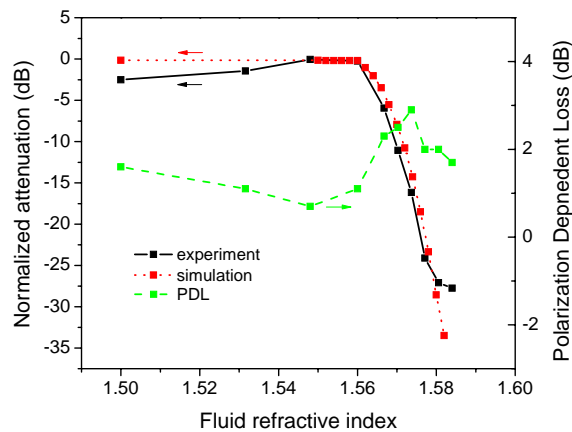


Fig. 3. Simulated and measured attenuation for the fabricated microfluidic variable optical attenuator. The dotted line is the simulation result and the solid line is the measured normalized attenuation for the device. The attenuation is the average of all polarization states. The dashed line is the PDL for the device.

The dashed line in Fig. 3 shows the polarization dependent loss (PDL), which we define as the maximum output power difference as we change the polarization state of the input signal through the paddle polarization controller. The measured device has a maximum PDL of 2.8 dB, which can be improved by a careful design of waveguide cross-section dimensions. Figure 4 shows the measured temporal response of the microfluidic VOA when the fluid index switches between 1.37 and 1.58. When we switch from one solution to another in the measurement, we just change to a different syringe with a different fluid. The switching time is around 2 micro seconds, but the power level fluctuates after the switching. The stabilization time of an output power variation less than 0.3dB is around 45 seconds after the cladding changes. Although we use immiscible fluids in the experiments, the later injected solution can not remove the former solution immediately due to the window opening under the channel, which causes an initial mixing of two fluids. An internal fluid control system with an

additional PMDS layer and a window opening with sloped sidewalls can reduce this fluctuation and shorten the stabilization time.

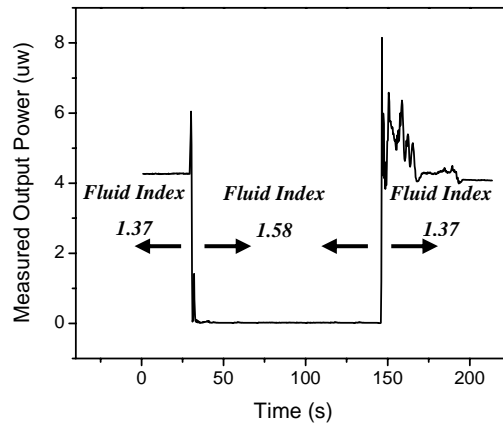


Fig. 4. Measured transient response for the fabricated microfluidic variable optical attenuator as the fluid refractive index changes between 1.37 and 1.58.

#### 4. Conclusion

In summary, we have demonstrated an effective method to integrate optical waveguides with microfluidic channels by introducing an opening in the cladding layer of optical waveguides. This integration method provides mechanically and chemically stable devices suitable for both optics and microfluidics applications. Based on the proposed fabrication process, we design and measure a microfluidic variable attenuator, achieving a maximum attenuation of 28 dB with a refractive index change of 0.027. In addition to the basic integration scheme discussed in this letter, the fabrication method also can be applied to large-scale integration of more complex planar waveguide circuits with microfluidic circuits.

#### Acknowledgments

The authors thank J. Poon for helpful discussions. Financial support from the National Science Foundation and Defense Advanced Research Projects Agency (Dr. D.Honey and Dr. R. Athale) is gratefully acknowledged.